

## Kamhi et al. Supplementary Material

### Plasmids

CAD constructs with mutated ATGs were prepared from CAD1 by the QuickChange PCR-based mutagenesis method (Stratagene) using the following sets of primers:

Primer 1[+] 5'- GCTCCGACCCACGGCGGCTCTGG -3'

Primer 1[-] 5'- CCAGAGCCGCCGTGGGGTTCGGAGC -3'

Primer 2[+] 5'- GGCCGGCACGGTTCGGCTACCCAGAGG -3'

Primer 2[-] 5'- CCTCTGGGTAGCCGACCGTGCCGGCC -3'

Primer 3[+] 5'- GCTGTGAAGGGGGGATAAGCGTGCGCTGG -3'

Primer 3[-] 5'- CCAGCGCACGCTTATCCCCCTTCACAGC -3'

Primer 4[+] 5'- CGCTGGGGTTGGGAGACGGCAGCGTATAAAGG -3'

Primer 4[-] 5'- CCTTATACGCTGCCGTCTCCCAACCCAGCG -3'

CAD1-Mut46 was prepared with primer sets 1-4; CAD1-Mut45 with primer sets 2-4; CAD1-Mut47 with primer sets 1, 3, 4; CAD1-Mut42 with primer sets 1, 2, 4; CAD1-Mut48 with primer sets 1-3. CAD1-Mut56 was prepared by mutagenesis of CAD1, using the following primers:

Primer 5[+] 5'- GCTTCTCTGTGCTCGCCTCGCCTCAGCTCCGACC -3'

Primer 5[-] 5'- GGTCGGAGCTGAGGCGAGGCGAGCACAGAGAAGC -3'

CAD1-Mut57 was prepared by mutagenesis of CAD1, using the following primers:

Primer 6[+] 5'- GGCTCTGGTGTGGAAGACGGGTCGGTGCTGC -3'

Primer 6[-] 5'- GCAGCACCGACCCGTCTTCCAACACCAGAGCC -3'.

### RT-PCR primers

CAD primer a [+] 5'- CTCAGATCCTGGTTCGACGGC -3';

CAD primer c [+] 5'- CCGGGTGCAGGAGTGACAGC -3';

CAD primer b [-] 5'- CAGGGAGCCGCACCAGTTTC -3';

CAD primer j [+] 5'- TCTGGTGTGAGGACGGGT -3';

CAD primer k [-] 5'- CTTGGTGACGAAGGAGGAAA -3';

CAD Pre-mRNA [+] 5'- AGAGAGGAGTTTACGTTGGGAGG -3';

CAD Authentic mRNA [+] 5'- ACCAAACTCTTCGTGGAGGCC -3';

CAD Latent mRNA [+] 5'- CCAGAGGCGGAGAGGCC -3'.

IDUA primer b [+] 5'-CGAGCACGCGTGGCCATGCGT-3';

IDUA primer c [-] 5'-AGGACGTAAGTGGTCAGCCTGG-3';

IDUA primer d [+] 5'-ACTGTGAGAGCTTCAGAGACC-3'

GFP [+] 5'- TGGAGAGGGTGAAGGTGATG -3';

GFP [-] 5'- AAGGGCAGATTGTGTGGAC -3';

$\beta$ -globin [+] 5' –AGGAGAAGTCTGCCGTTAC – 3';

$\beta$ -globin [-] 5' –CCTGAAGTTCTCAGGATCC – 3';

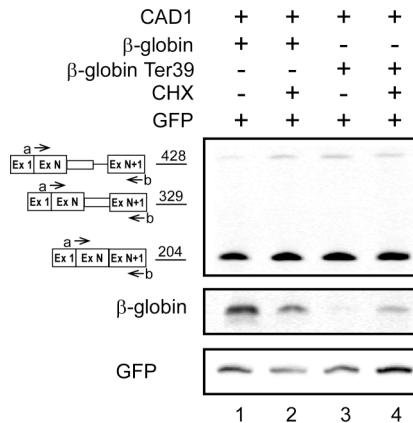
$\beta$ -actin [+] 5' – CTGGAACGGTGAAGGTGACA – 3';

$\beta$ -actin [-] 5' – AAGGGACTTCCTGTAACAATGCA – 3';

hUpf1 [+] 5'-AGGCCATCGACTCCCCGGTGTCTTT-3';

hUpf1 [-] 5'-GTAGAAGATGTTGGATGGGAAGGCG-

## Supplementary Figure 1S



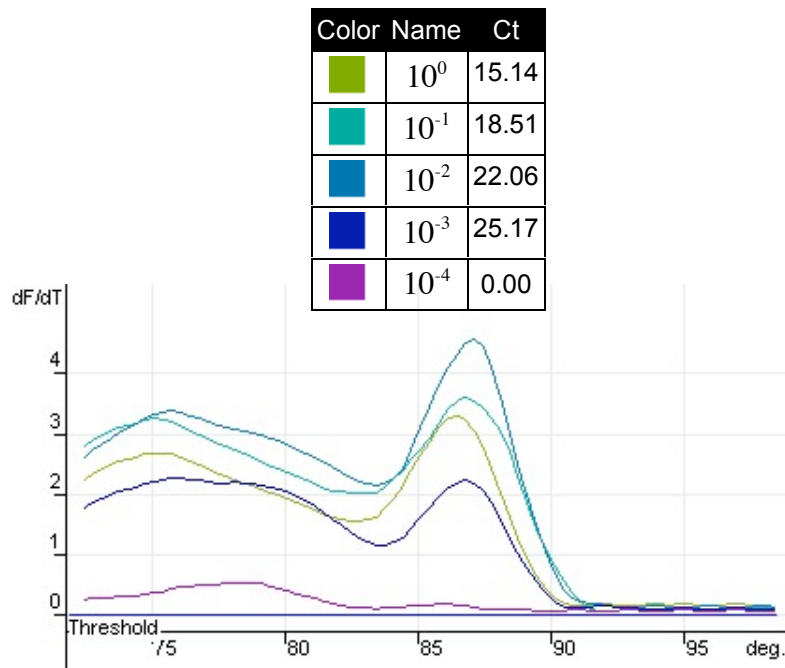
**Supplementary Figure 1S.** Abrogation of NMD does not elicit latent splicing in the wild-type CAD1 pre-mRNA. Human 293T cells were cotransfected with the indicated plasmids and treated with 20  $\mu$ g/ml of CHX for 2 hr (lanes 2 and 4).  $\beta$ -globin, wild type  $\beta$ -globin;  $\beta$ -globin Ter39, a mutant construct expressing  $\beta$ -globin mRNA having a PTC at position 39; CAD1, wild-type CAD1. The splicing patterns of CAD1,  $\beta$ -globin and GFP were revealed by RT-PCR. Abrogation of NMD by the CHX treatment is evidenced by the upregulation of  $\beta$ -globin Ter39 mRNA (compare lanes 3 and 4) whereas latent splicing in CAD1 mRNA is not elicited by this treatment (lanes 2 and 4).

## Supplementary Figure 2S

### Sensitivity of detection of latent splicing

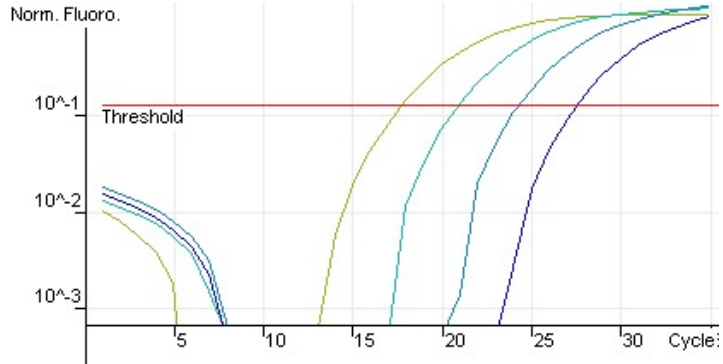
Because we could not detect any latent mRNA from the wild-type constructs (harboring in-frame stop codons upstream of the latent 5' splice site), we further evaluated the sensitivity of the real-time RT-PCR procedure. To this end we analyzed the presence of latent mRNA in a serial dilutions of RNA expressed from CAD2 Mut1, a construct already established for the expression of latent mRNA. As can be seen in the dissociation curve in Figure 2Sa, all reactions except for the  $10^{-4}$ -sample, produced one product corresponding to the latent mRNA. The amplification reactions were monitored (Figure 2Sb I) and plotted to create a standard curve based on the relative expected levels of latent mRNA, as predicted for the serial dilutions (Figure 2Sb II). The color code and Ct values are presented in the table inserted in Figure 2SaTable S2-1.

This experiment shows that quantities 4 orders of magnitude less than the level calculated for CAD2-Mut1 can be detected. Hence, we use the term “fully suppressed” to indicate that quantitative RT-PCR analyses did not detect latent mRNA in the wild-type constructs (containing stop codons).

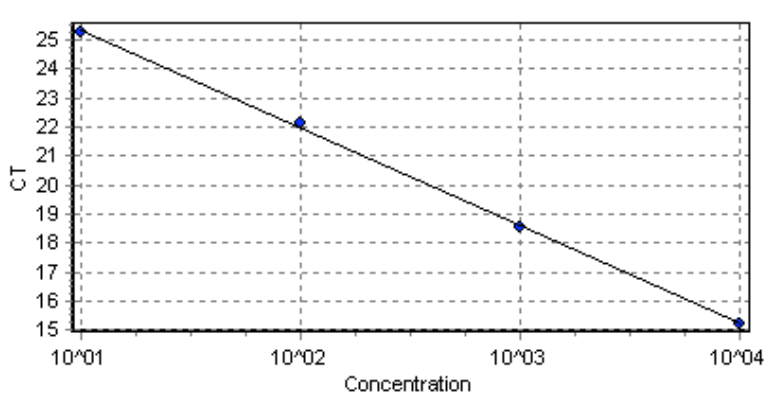


**Supplementary Figure 2Sa.** Dissociation curve of the real-time RT-PCR reaction of the serially diluted samples derived for CAD2-Mut1. Color code and Ct values are presented in the table.

I

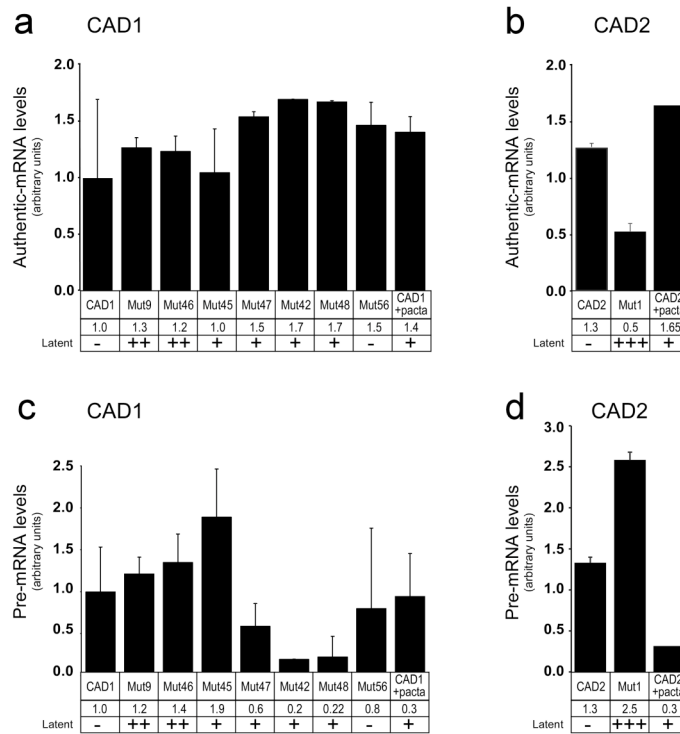


II

**Figure 2Sb. Quantitation data for cycling of CAD2-Mut1 serial dilution**

Serial dilutions of the cDNA from CAD2 Mut1 mRNA were carried out as described above, and fluorescence was analyzed and plotted to a log scale. The fluorescence readings were then used to produce a standard curve to verify the reaction efficiency and accuracy of the dilution steps. The resulting efficiency was 1.98, the slope -3.363 and  $R^2$  is 0.99933.

## Supplementary Figure 3S



**Supplementary Figure 3S. Quantitative analyses of the effect of start codons- or intronic stop codons-removal on levels of authentic and precursor CAD mRNAs.** (a, b) Levels of authentic mRNAs expressed from the wild-type CAD1 (a) and CAD2 (b) constructs, as well as from the respective mutants derived from them, were calculated by normalizing the fluorescence reading levels obtained from PCR reactions using “Authentic/b” primer pair, to the integrated total RNA reading (The level of CAD1 set as 1.00). (c, d) Levels of pre-mRNAs expressed from the same constructs as above were calculated by normalizing the fluorescence reading levels obtained from PCR reactions using “Pre-mRNA/b” primer pair to the integrated total RNA reading (The level of CAD1 set as 1.00). These comparisons show that the levels of authentic mRNAs do not fluctuate dramatically among the various constructs, and that the accumulation of pre-mRNAs cannot be correlated with the occurrence of latent splicing. Columns are marked with the construct name (upper row), the normalized level of the measured RNA (middle row), and the absence (-) or occurrence (+) of latent splicing (lower row).